



ELSEVIER

Journal of Chromatography A, 687 (1994) 201–212

JOURNAL OF
CHROMATOGRAPHY A

Properties of some C_{18} stationary phases for preparative liquid chromatography

II. Column efficiency

Hong Guan^{a,b}, Georges Guiochon^{a,b,*}

^aDepartment of Chemistry, University of Tennessee, Knoxville, TN 37996-1600, USA

^bDivision of Chemical and Analytical Sciences, Oak Ridge National Laboratory, Oak Ridge, TN 37831-6120, USA

First received 17 May 1994; revised manuscript received 10 August 1994

Abstract

Apparent column efficiencies were measured for 2,6-dimethylphenol, 3-phenyl-1-propanol, *m*-cresol and methyl benzoate on six columns packed with two commercial octadecyl silica, using methanol-water solutions as the mobile phase. The columns having the less dense packing are also the most efficient (the long-term stability problem conventionally associated with low packing-density columns has not been studied). The dependence of the column efficiency on the sample size is well accounted for by the Knox-Pyper model, using the isotherm data previously determined and the solution of the ideal model to account for the thermodynamic contribution to band broadening.

1. Introduction

In a companion paper [1], we discussed the results of measurements of isotherm data for 2,6-dimethylphenol, 3-phenyl-1-propanol and methyl benzoate on six different columns prepared with two different octadecyl silica adsorbents for reversed-phase liquid chromatography. The first two components give Langmuirian isotherms on both stationary phases, the last one gives an anti-Langmuirian isotherm. Calculated and measured band profiles were generally in good agreement, showing that the model errors

have been properly corrected or accounted for.

For each component, the same isotherm model could be used to account for the adsorption data on the different columns, the Langmuir model for the first two compounds, the quadratic model for the last one. The parameters of these isotherms are quite different on the two stationary phases. For each stationary phase, the parameters determined for each column are somewhat different, but most of the differences can be explained by the differences in density of the column packing.

The aim of the present paper is to compare the efficiency data acquired in the same time on the different columns studied, and the dependence of the apparent column efficiency on the sample size.

* Corresponding author. Address for correspondence: Department of Chemistry, University of Tennessee, Knoxville, TN 37996-1600, USA.

2. Theory

Classically, the column efficiency is a measure of the relative bandwidth of elution peaks

$$N_0 = 5.54 \cdot \left(\frac{t_R}{W_{0.5}} \right)^2 \quad (1)$$

where N_0 is the number of theoretical plates of the column, t_R is the retention time of the peak and $W_{0.5}$ is its width at half height. In linear chromatography, the column efficiency is simply related to the design and operation parameters of the column. In non-linear chromatography, the apparent efficiency is also a function of the sample size.

The column efficiency has also been related to the second statistical moment of the band, proportional to the band variance. The definitions are equivalent for nearly symmetrical peaks. Column efficiency being an empirical parameter [2], the choice is a matter of convenience. With the protocol defined in the Experimental section, the precision obtained by measuring the width at half height (ca. 1%) is an order of magnitude better than could be achieved for the determination of the second moment because of the uncertainty, due to the signal noise, regarding the time when the integration should be stopped.

2.1. Linear chromatography

In linear chromatography, the elution bandwidth observed for small samples injected in a short time depends only on the axial dispersion and on the mass-transfer kinetics. A correlation between the height equivalent to a theoretical plate (HETP: $H = L/N_0$, with $L =$ column length), which characterizes the relative bandwidth, and the mobile phase flow velocity (u) has been described by Done et al. [3] who defined the *reduced plate height* h as

$$h = \frac{H}{d_p} \quad (2)$$

and the *reduced velocity* ν or particle Peclet number (see [4]) as

$$\nu = \frac{d_p u}{D_m} \quad (3)$$

where d_p is the average diameter of the packing particles and D_m is the diffusion coefficient of the compound in the mobile phase. The universal correlation is given by

$$h = \frac{b}{\nu} + a\nu^n + c\nu \quad (4)$$

where b characterizes axial diffusion, due to the concentration gradient along the column axis, at the boundaries of the band, a the eddy diffusion, a function of the homogeneity of the column packing, and c the mass-transfer kinetics. The exponent n is commonly assigned a value of 1/3 to best fit experimental results [3]. The Knox equation predicts that the column efficiency reaches a maximum at a certain flow velocity, i.e., that there is a minimum in the h vs. ν plot.

2.2. Apparent efficiency in overloaded elution

In non-linear chromatography, the bandwidth depends also on the thermodynamics of phase equilibrium. Knox and Pyper [5] have suggested that the kinetic contribution to the column efficiency (due to axial dispersion and to mass-transfer resistances) can be separated from the thermodynamic contribution (due to the non-linear behavior of the equilibrium isotherm). This assumes that the mass-transfer resistances are independent of the solute concentration [2].

With this assumption, the apparent column efficiency, N , under overloaded conditions is given by

$$N = \frac{N_0 N_{th}}{N_0 + N_{th}} = \frac{N_0}{1 + \frac{N_0}{N_{th}}} \quad (5)$$

where N_0 refers to the column efficiency at infinite dilution (i.e., it is the plate number resulting from axial dispersion and the mass-transfer kinetics only, as given by Eq. 4) and N_{th}

Table 1
Column hold-up times and capacity factors

	Columns ^a					
	YS	YL	VS1	VS2	VL1	VL2
t_0 (min)	1.26	2.95	1.25	1.30	2.95	2.95
MC: k'	5.60	6.15	3.70	3.60	4.0	4.1
PP: k'	9.7	9.8	6.5	6.3	7.1	7.2
DMP: k'	11.2	12.1	7.1	7.0	7.9	8.1
MB: k'	13.2	14.1	8.8	8.6	9.8	10.3

MC = *m*-Cresol; PP = 3-phenyl-1-propanol; DMP = 2,6-dimethylphenol; MB = methyl benzoate.

^aAll columns, I.D. 4.6 mm. YS: $L = 10$ cm, YMC ODS; YL: $L = 25$ cm, YMC ODS; VS1: $L = 10$ cm, Vydac ODS; VS2: $L = 10$ cm, Vydac ODS; VL1: $L = 25$ cm, Vydac ODS; VL2: $L = 25$ cm; Vydac ODS.

is the apparent plate number of an infinitely efficient column at finite concentration, resulting from the non-linear behavior of the isotherm. N_{th} can be derived from the band profile calculated in ideal chromatography [2]. It is given by

$$N_{th} = 5.54 \cdot \frac{(2 - L_r^{1/2})^4}{(4L_r^{1/2} - L_r)^2} \cdot \left[1 + \frac{t_p + t_0}{k'_0 t_0} \cdot \frac{1}{(1 - L_r^{1/2})^2} \right]^2 \quad (6)$$

where t_p is the duration of the injection, k'_0 is the limit retention factor of the component (or retention factor at infinite dilution) and L_r its loading factor, defined as the ratio of the amount of component injected to the column saturation capacity for that component:

$$L_r = \frac{n}{q_s} = \frac{nb}{SLk'} \quad (7)$$

where n is the amount of component injected, S and L are the column geometrical cross-section area and length, respectively, and b is the second coefficient of the Langmuir equation. The loading factor as defined above is meaningless for an isotherm which has no horizontal asymptote.

The dependence of the apparent column efficiency on the sample size has been discussed previously, using the theoretical approach outlined above [2,6,7] or a more empirical method

[8,9]. Lucy and Carr [7] have shown that, in spite of some fundamental reservations [10], the method gives correct results at moderate and high loading factors, a result also in agreement with experimental determinations [6].

3. Experimental

The same equipment (Perkin-Elmer, Norwalk, CT, USA), the same columns, the same chemicals and the same procedures were used in this work as in the work described in the companion paper [1], except that column efficiencies were also measured for *m*-cresol, 99%, liquid (Aldrich, Milwaukee, WI, USA), formula weight (FW) 108.14 [CAS Ref. No. 108-39-4], catalog No. C8,572-7. Solutions of *m*-cresol with concentrations between 172.5 and 4.22 mg/ml were prepared.

3.1. Measurement of the column efficiency

To determine the efficiency under linear conditions, the retention times and bandwidths at half height were measured as a function of the flow velocity for the four components using the most dilute solutions prepared, to avoid column overloading. The choice of measuring the band width at half height rather than at the baseline or

any other fractional height is arbitrary. From previous, independent studies [11], however, the width at half height seems to afford the most precise measurement of the column bandwidth. It is also readily amenable to automatic determination using a simple calculation procedure.

At each flow-rate, a 0.010-ml (for 10 cm long columns) or a 0.020-ml (for 25 cm long columns) sample was injected. The calibration curves reported independently [1] were used. Apparent efficiencies under overloaded conditions were determined following the same procedure, but using larger volume loops and more concentrated solutions, as needed.

The retention data under linear conditions are listed in Table 1. The other column characteristics are reported in the companion paper [1], Table 1.

3.2. Numerical treatment of the data

The determination of the column efficiency from recorded experimental band profiles requires the measurement of the retention time and the bandwidth at half height (Eq. 1). To reduce the contribution of the experimental errors and particularly that of the signal noise and of a non-linear detector response, the following procedure was used. First, the chromatograms [1] were transformed from records of the detector output (i.e., electrical voltage) versus the running time into plots of component con-

centration in the mobile phase, C , versus time t . Second, the data points in the following three groups were extracted into separate files.

Group I contains all the data points ranging between 90 and 100% of the peak maximum and will be processed to derive the retention time of the peak and its height. Groups II and III contain the data points ranging between 45 and 55% of the peak maximum, with the signal increasing or decreasing with increasing time, respectively. They will be processed together to derive the bandwidth at half height.

The data points of the first group are fitted to a parabolic model

$$C = a_2 t^2 + a_1 t + a_0 \quad (8)$$

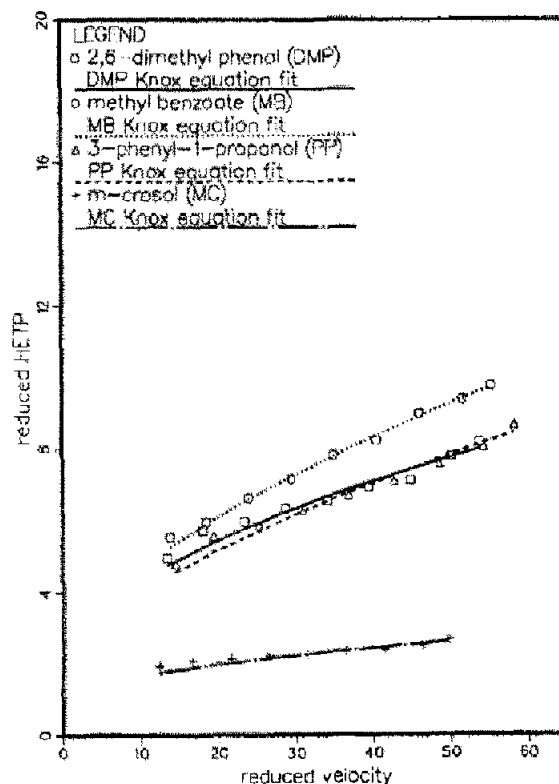


Fig. 1. Comparison between the experimental data for the column efficiency (symbols) and the best fit to the Knox equation (lines). Column YS ($L = 10$ cm, YMC ODS).

Table 2
Parameters used in the Wilke-Chang equation

	Compounds			
	MC	DMP	PP	MB
M_A (g/mol)	108.1	136.2	122.2	136.1
d_A (g/ml)	1.034	1.001	1.025	1.094
V_A (ml/mol)	104.6	136.1	119.2	124.5
$D_m \times 10^6$	6.06	5.17	5.60	5.46

For compound abbreviations, see Table 1.

Table 3
Calculated coefficients for the Knox equation

Sample	Coefficient	Columns					
		YS	YL	VS1	VS2	VL1	VL2
MC	<i>a</i>	0.71	1.80	0.81	0.45	1.87	1.88
	<i>c</i>	0.000	0.000	0.006	0.099	0.003	0.000
DMP	<i>a</i>	1.60	2.88	2.88	1.94	2.85	2.55
	<i>c</i>	0.038	0.000	0.002	0.029	0.059	0.012
PP	<i>a</i>	1.85	3.18	2.70	2.11	3.56	2.82
	<i>c</i>	0.018	0.000	0.015	0.008	0.012	0.000
MB	<i>a</i>	1.89	2.50	2.03	2.48	2.43	2.17
	<i>c</i>	0.045	0.078	0.035	0.000	0.018	0.030

For columns and compound abbreviations, see Table 1.

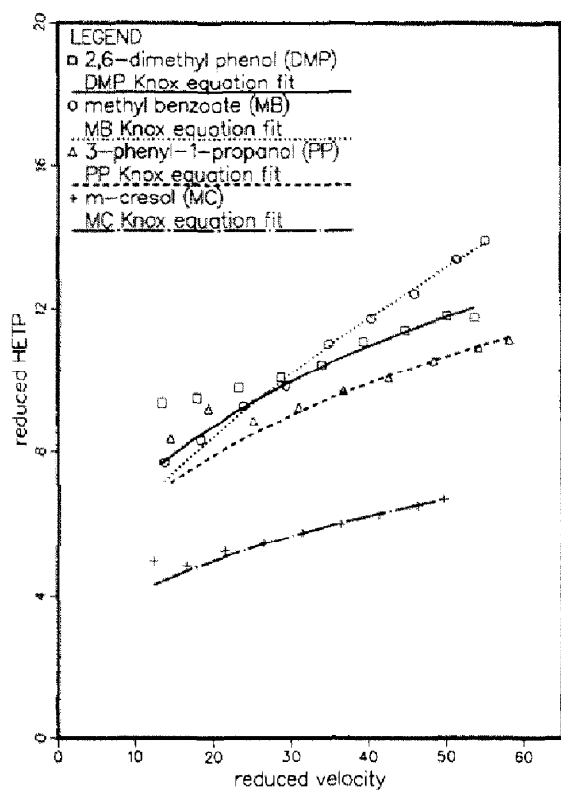


Fig. 2. Same as Fig. 1, but column YL ($L = 25$ cm, YMC ODS).

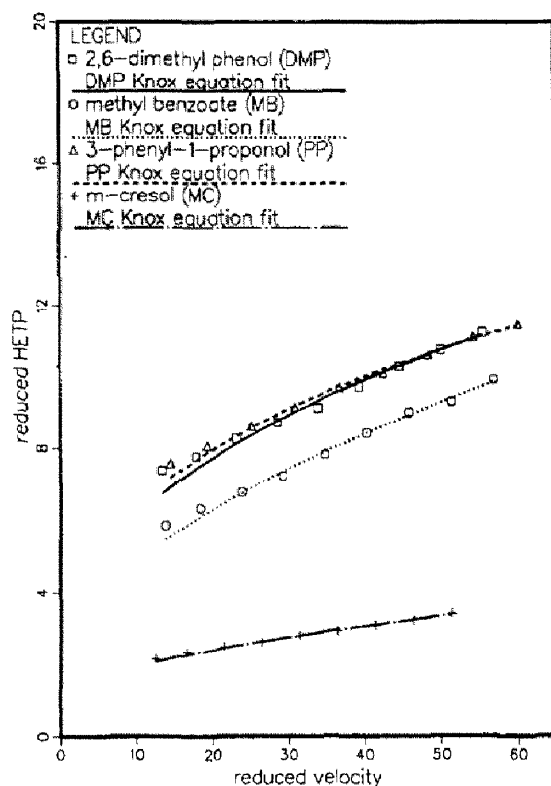


Fig. 3. Same as Fig. 1, but column VS1 ($L = 10$ cm, Vydac ODS).

using a least-square method. From the best coefficients a_2 , a_1 and a_0 the coordinates of the peak maximum, hence the retention time, t_R and the maximum concentration of the peak, C_M , are calculated.

The data points of each of the other two groups are fitted to a linear equation

$$C = b_1 t + b_0 \quad (9)$$

Using the best values of the coefficients b_1 and b_0 , the times corresponding to the elution of the concentration $C_M/2$ on each side of the band are determined by interpolation. This gives the bandwidth at half height.

This procedure of data smoothing is carried out entirely by software which eliminates human

judgment and errors and ensures the maximum reproducibility.

3.3. Determination of the reduced velocity

Finally, the mobile phase flow velocity was measured as $u = L/t_0$, with L = column length and t_0 = retention time of uracil. For all compounds, this velocity is converted into a reduced velocity, using Eq. 3, with the known particle size (10 μm) and the diffusion coefficients derived from the classical Wilke and Chang equation [12]

$$D_{A,B} = 7.4 \cdot 10^{-8} \cdot \frac{\sqrt{\psi_B M_B T}}{\eta_B V_A^{0.6}} \quad (10)$$

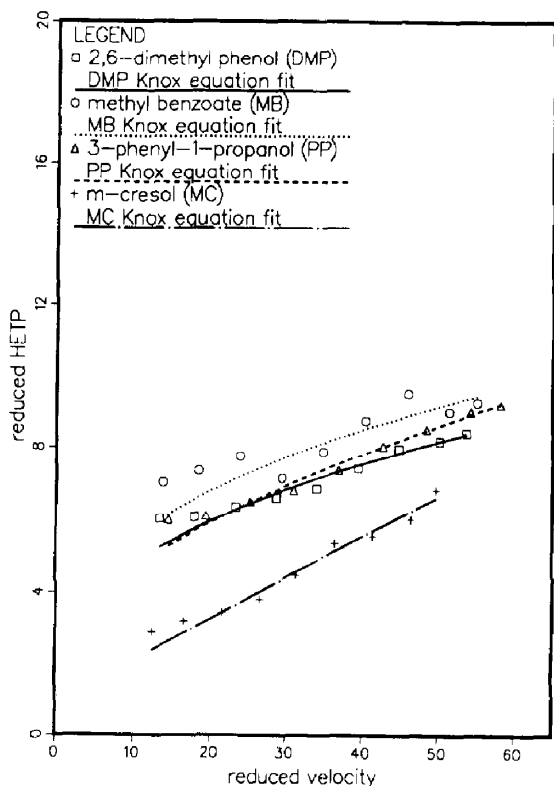


Fig. 4. Same as Fig. 1, but column VS2 ($L = 10$ cm, Vydac ODS).

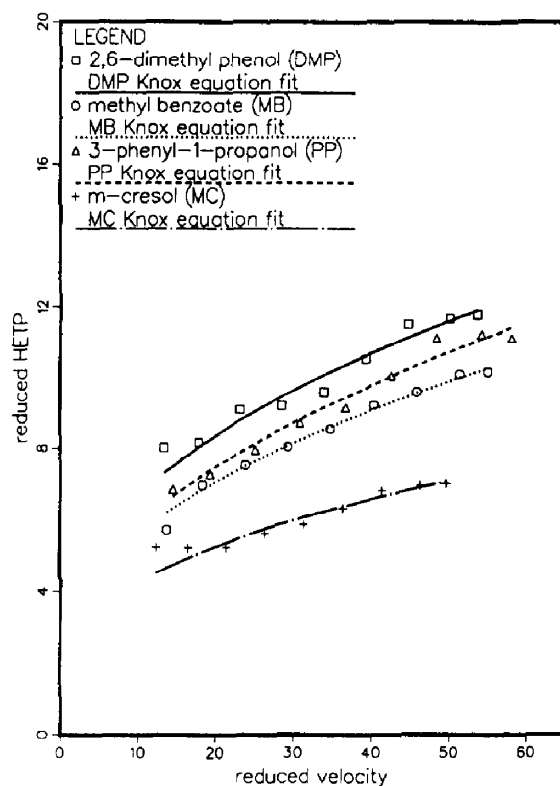


Fig. 5. Same as Fig. 1, but column VL1 ($L = 25$ cm, Vydac ODS).

where ψ_B is an association constant for the solvent, M_B is the molecular mass of the solvent (g/mol), η_B its viscosity (cP), V_A the molar volume (ml/mol) of the liquid solute at its normal boiling point, and T the absolute temperature (K). Recommended ψ_B values are 1.9 for methanol and 2.6 for water [12]. The value for V_A can be calculated from group contributions [13,14]. Since the solvent used is a solution of methanol–water (40:60) ($M_{\text{methanol}} = 32.04$ g/mol, $M_{\text{water}} = 18.00$ g/mol), the value of $\psi_B M_B$ was taken as the weighed average, i.e.

$$\psi_B M_B = 60\% \psi_{\text{water}} M_{\text{water}} + 40\% \psi_{\text{methanol}} M_{\text{methanol}} = 52.4304 \quad (11)$$

Temperature T was taken as 298.13 K and the solvent viscosity 1.62 cP [2]. The value of V_A for

each compound studied was taken as the quotient of that molecular mass M_A divided by its density d_A . The data used are summarized in Table 2.

3.4. Representation of the efficiency data

The values of the reduced efficiency and reduced velocity are fitted to the Knox equation [3] using a linear regression and setting $b = 1.5$ for the lack of data at low values of the reduced efficiency. In a few instances, this procedure leads to negative values of c , in which case c was set to 0 and the procedure repeated for the determination of a . The coefficients obtained are reported in Table 3 and used to draw the lines in the figures.

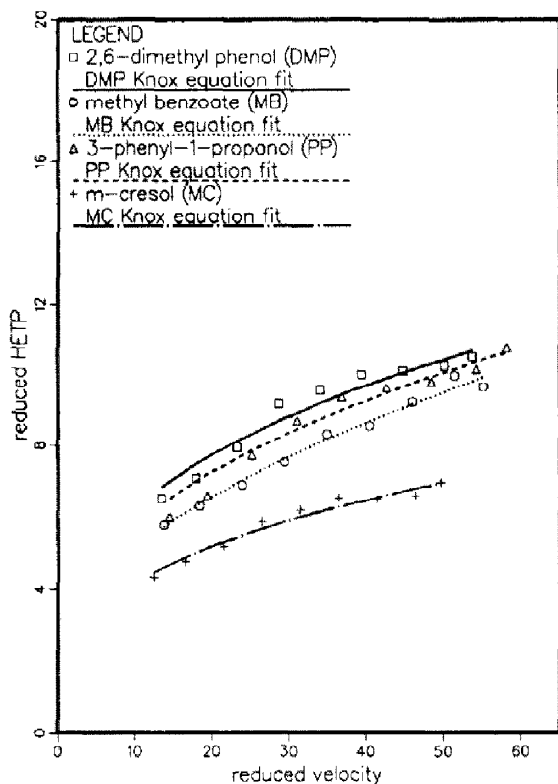


Fig. 6. Same as Fig. 1, but column VL2 ($L = 25$ cm, Vydac ODS).

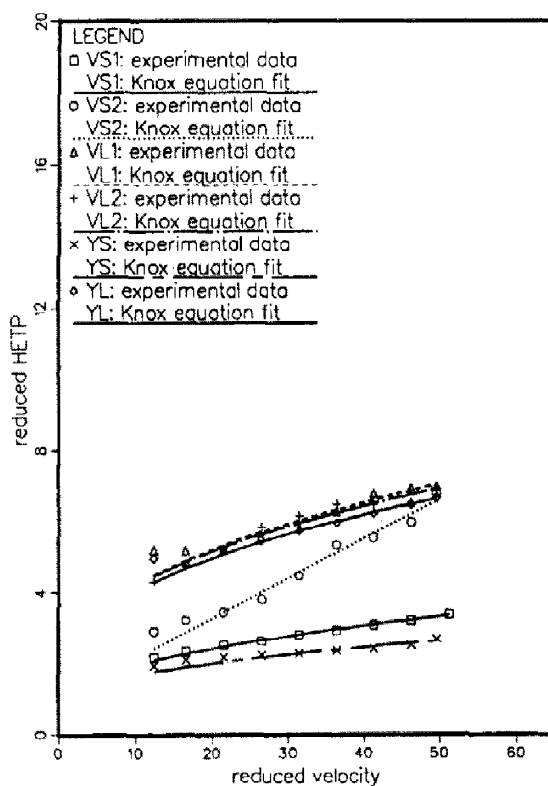


Fig. 7. Comparison between the experimental data for column efficiency (symbols) and the best fit to the Knox equation (lines). Data for *m*-cresol.

4. Results and discussion

4.1. Effect of the mobile phase flow-rate on the column efficiency

The experimental results are shown in Figs. 1–6 (symbols) as plots of the reduced HETP versus the reduced velocity for the six columns studied. No data were collected in the velocity range where axial dispersion controls the band width because this effect is well known. We are mainly interested in the mass-transfer resistances which constitute the main contribution to band broadening at the high flow velocities at which preparative columns must be operated. So no minima are observed on the curves. In all cases, the reduced efficiency increases with increasing reduced velocity in a manner consistent with the Knox equation (Eq. 4). As expected, there is a

good agreement between the experimental data points (symbols) and the curves derived from the best coefficients obtained by fitting these results to the Knox equation (Table 3).

Two different trends are observed when comparing the data in Tables 1 and 3 and in Figs. 1–6. For the three components (*m*-cresol, 3-phenyl-1-propanol and 2,6-dimethylphenol) whose adsorption follows Langmuir behavior, the reduced plate height increases with increasing capacity factor k' , leveling at high values: on any given column, there is little difference between the efficiencies for 3-phenyl-1-propanol and 2,6-dimethylphenol. On the other hand, the column efficiency for methyl benzoate does not seem to depend on its retention factor.

The reproducibility of efficiency data on any single column is excellent. For example, based on six measurements done with *m*-cresol, the

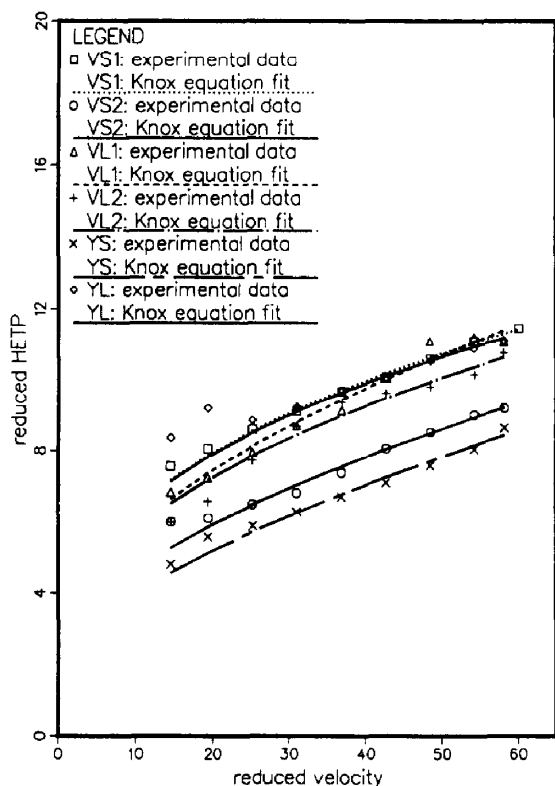


Fig. 8. Same as Fig. 7, except data for 3-phenyl-1-propanol.

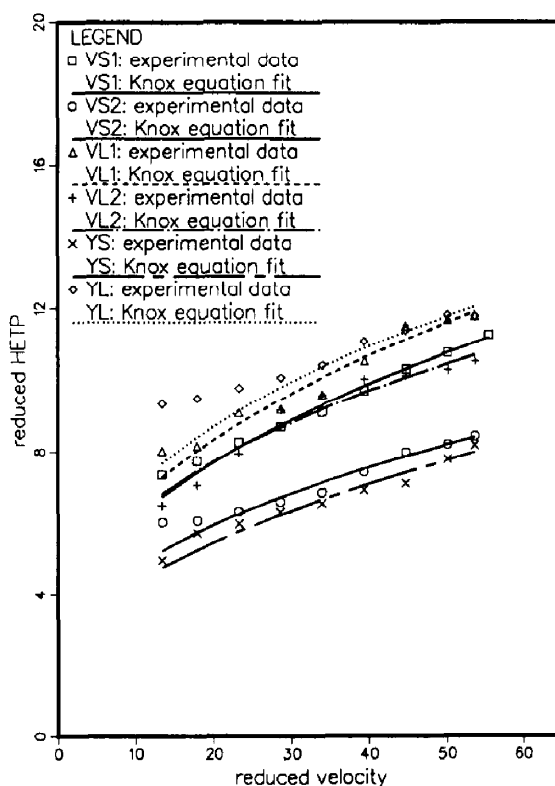


Fig. 9. Same as Fig. 7, except data for 2,6-dimethylphenol.

relative standard deviation (R.S.D.) on the HETP is 1%. This is in large part because of the rigorous procedure adopted for the determination of the width at half height (R.S.D. of $W_{0.5}$, 0.4%), the column-to-column reproducibility is not necessarily so and deserves a more detailed study. While Figs. 1-6 showed the efficiency data obtained on each column and revealed interesting trends regarding the dependence of the efficiency on the retention factor, Figs. 7-10 show the same data for each component and permit a comparison of the performance of the different columns.

The data in Table 3 confirm that the Knox equation (Eq. 4) is an empirical correlation, not the mathematical expression of a rigorous model based on first principles. This is clear from the origin of this equation [2] and was explained by Done et al. [3]. The constant a characterizes

eddy diffusion and the lack of homogeneity of the packing. On this basis, the values of a on a given column, for compounds which have very similar diffusivities (Table 2) are expected to be very close. As seen in Table 3, they are not but, depending on the column, vary as 1 to 1.5 (VL2) or 1 to 5 (VS2). Similarly, c characterizes the mass-transfer kinetics through the particles. The values of c for a given compound should be the same on a given packing material since column-to-column variations in the packing density should not affect mass transfer inside particles. Nevertheless, c varies from column to column for a given component.

The general conclusion is that the data obtained with a given stationary phase are poorly

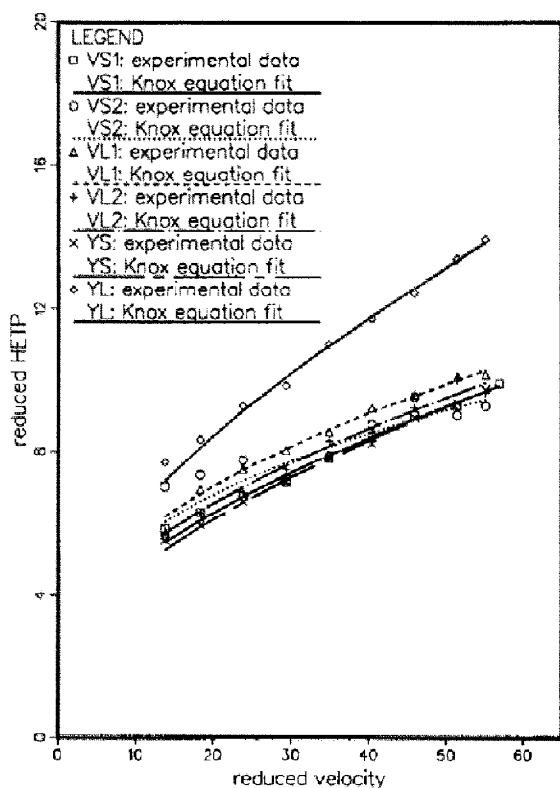


Fig. 10. Same as Fig. 7, except data for methyl benzoate.

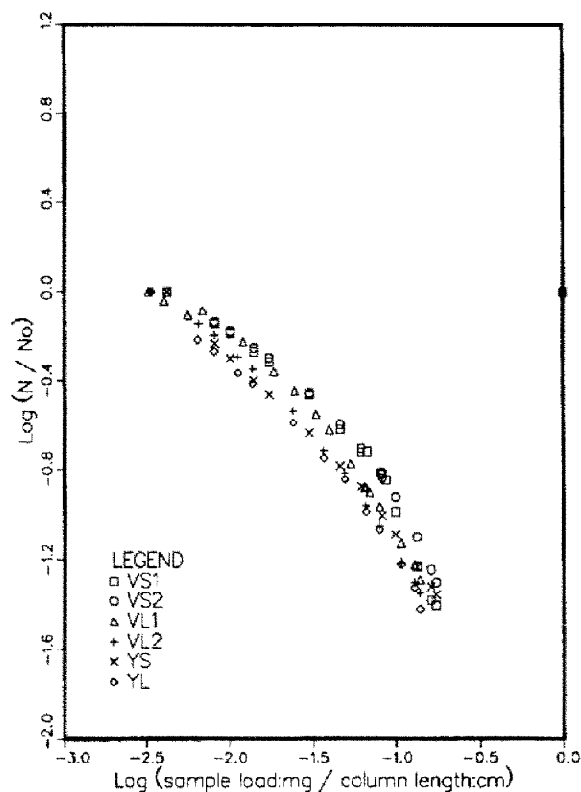


Fig. 11. Plot of the logarithm of the ratio of the apparent column efficiency (N) and the column efficiency at zero-sample size (N_0) vs. the logarithm of the ratio of the injected sample (mg) and the column length (cm) for *m*-cresol.

reproducible from column to column, which is most probably related to the packing procedure employed and must be correlated with the fluctuations of the packing density previously reported. The scattering of the curves obtained does not seem to depend on the nature of the packing material used. However, it seems that the short columns (10 cm long) tend to have lower reduced plate heights than the long ones (25 cm long) for all the compounds studied, effectively pointing to a packing problem. It should not be concluded hastily, however, that a low packing density should be preferred. First, the experimental results presented here are insufficient to warrant a strong correlation between column efficiency and packing density. Second, there are some serious doubts regarding the long-term stability of columns which have a low packing density. Under the influence of a constant stream of eluent, slow consolidation of the packing is bound to take place.

4.2. Apparent column efficiency and sample size

The apparent column efficiency was measured as a function of the amount of sample injected at a constant flow-rate of 1.0 ml/min. The data are plotted (Figs. 11-14) in logarithmic coordinates. In order to eliminate the trivial effect of the column length, the logarithm of the ratio of the column efficiency to its limit efficiency at zero sample size is plotted versus the logarithm of the ratio of the sample size to the column length. The logarithm of the loading factor would be more appropriate for compounds with a Langmuir adsorption isotherm, but there is no saturation capacity for an anti-Langmuir isotherm.

The behavior of the components whose adsorption follows a Langmuirian isotherm (Figs. 11-13) is strikingly different from that of methyl benzoate (Fig. 14) which has an anti-Langmuirian isotherm. For the first three compounds, the column efficiency decreases monotonically

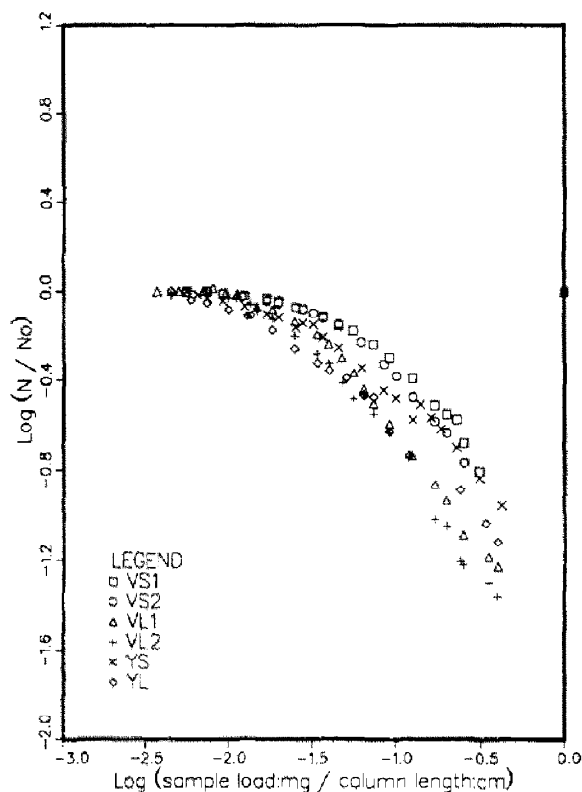


Fig. 12. Same as Fig. 11, except 3-phenyl-1-propanol.

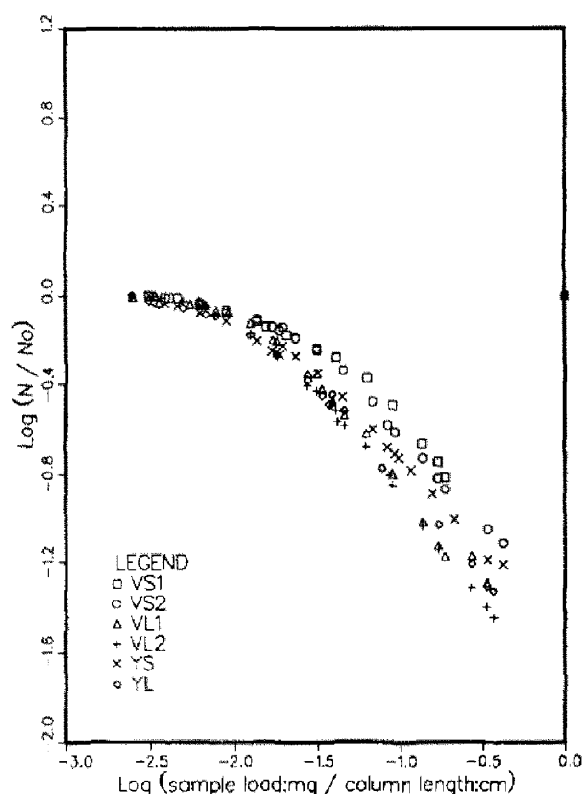


Fig. 13. Same as Fig. 11, except 2,6-dimethylphenol.

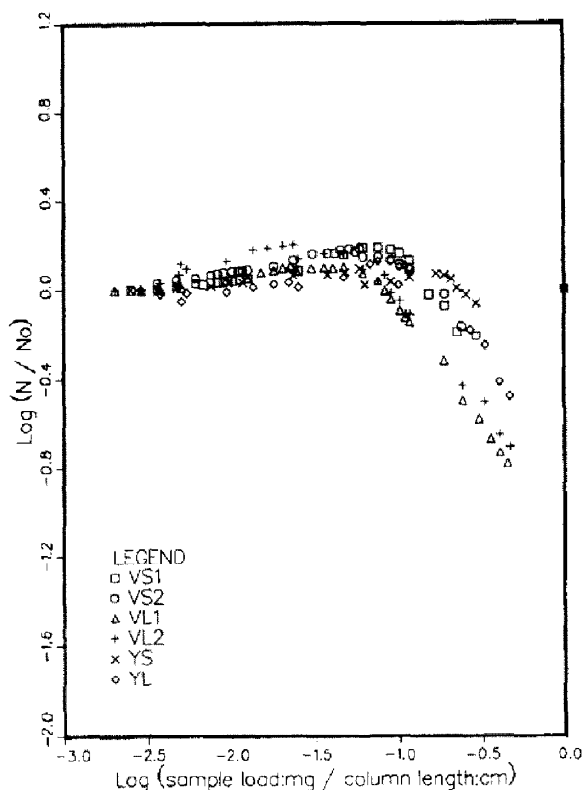


Fig. 14. Same as Fig. 11, except methyl benzoate.

with increasing sample amount. For the last one, the efficiency begins to increase at low sample sizes and goes through a maximum. This anomalous behavior is explained by the initial increase in the retention time of methyl benzoate when the sample amount is increased. Note that for *m*-cresol it was not possible to make a precise measurement of the column efficiency at a sample size small enough to ensure linear behavior of the retention mechanism.

Using the model of Knox and Pyper [5] described in the Theory section and the band profile given by the ideal model, it is possible to account simply for these results in the case of the compounds whose adsorption behavior follows the Langmuir model [5,6]. Because the width of a Gaussian profile and that of an ideal model profiles are related to the fractional height in a different way, different equations must be used, depending on which fractional height is used.

The width at half height can be measured with better accuracy and precision than the baseline width and has been used here. Golshan-Shirazi and Guiochon [6] have shown that, in the case of a component following the Langmuir adsorption model, the thermodynamic contribution to the column efficiency is given by Eq. 6. When the loading factor is moderate, this equation can be simplified and becomes

$$N_{th} = \frac{5.54}{L_f} \cdot \left[\frac{1+k'_0}{k'_0} \right]^2 \cdot \left[1 + \left(2.5 - \frac{4k'_0}{1+k'_0} \right) \cdot \sqrt{L_f} \right] \quad (12)$$

In Figs. 15 and 16 the experimental results (symbols) obtained with the different columns

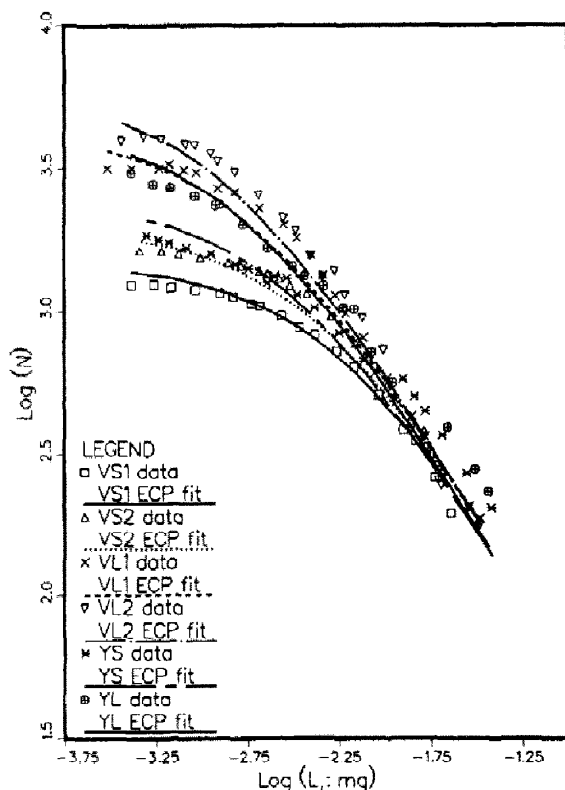


Fig. 15. Comparison between experimental results and theoretical dependence of the column efficiency on the sample size. 3-Phenyl-1-propanol.

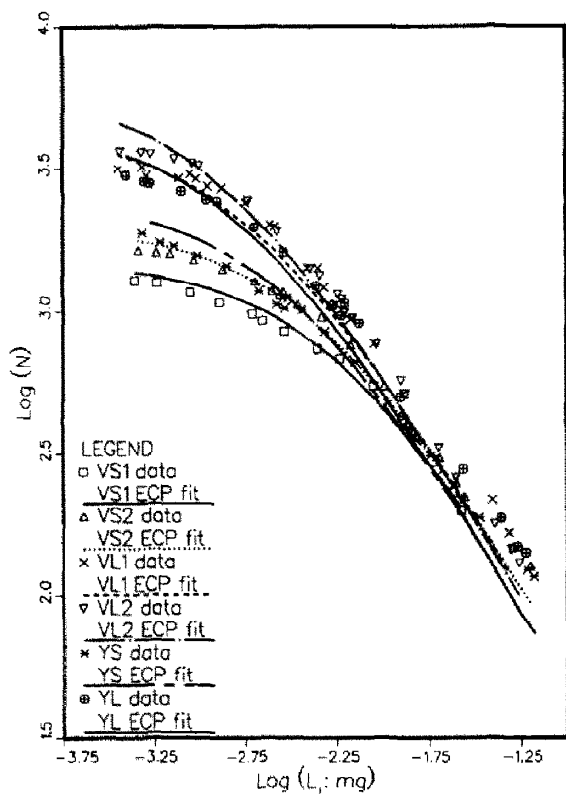


Fig. 16. Same as Fig. 15, except 2,6-dimethylphenol.

Acknowledgements

We acknowledge the gift of samples of stationary phases by YMC and Vydac. This work was supported in part by grant CHE-9201663 from the National Science Foundation and by the cooperative agreement between the University of Tennessee and the Oak Ridge National Laboratory. We acknowledge support of our computational effort by the University of Tennessee Computing Center.

References

- [1] H. Guan and G. Guiochon, *J. Chromatogr. A*, 687 (1994) 179.
- [2] G. Guiochon, S. Golshan-Shirazi and A.M. Katti, *Fundamentals of Preparative and Nonlinear Chromatography*, Academic Press, Boston, MA, 1994.
- [3] J.N. Done, G.J. Kennedy and J.H. Knox, in E.S. Perry (Editor), *Gas Chromatography 1972*, Applied Science, London, 1973, p. 145.
- [4] J.C. Giddings, *J. Chromatogr.*, 13 (1964) 301.
- [5] J.H. Knox and H.M. Pyper, *J. Chromatogr.*, 363 (1986) 1.
- [6] S. Golshan-Shirazi and G. Guiochon, *Anal. Chem.*, 60 (1988) 2364.
- [7] C.A. Lucy and P.W. Carr, *J. Chromatogr.*, 556 (1991) 159.
- [8] H. Colin, *Sep. Sci. Technol.*, 22 (1987) 1953.
- [9] N.T. Miller, *J. Chromatogr.*, 550 (1991) 301.
- [10] E.V. Dose and G. Guiochon, *Anal. Chem.*, 62 (1990) 1723.
- [11] D.L. Ball, W.E. Harris and H.W. Habgood, *J. Gas Chromatogr.* 5 (1966) 613.
- [12] C.R. Wilke and P. Chang, *AIChE J.*, 1 (1955) 264.
- [13] R.C. Reid, J.M. Prausnitz and B.E. Poling, *The Properties of Gases and Liquids*, McGraw-Hill, New York, 4th ed., 1987.
- [14] A.L. Hines and R.N. Maddox, *Mass Transfer: Fundamentals and Applications*, Prentice-Hall, Englewood Cliffs, NJ, 1985.

for 3-phenyl-1-propanol and 2,6-dimethylphenol have been replotted as $\log N$ versus $\log L_t$, using the equilibrium isotherm data determined in the companion paper to calculate L_t . The values calculated from Eq. 12 are also given (lines). There is an excellent general agreement between the theoretical prediction and the experimental results. The deviations observed at high values of the loading factor are due to inaccuracies in the estimate of the width of the injection (i.e., of t_p in Eq. 6), which is neglected in Eq. 12, although it becomes significant for large sample sizes.